ISSN 2395-1621

Computational Fluid Dynamics Optimization of Roof Curvature for Drag Reduction of Passenger Car

[#1]Ravindra A. Viveki, [#2]Dr.N.K.Chougule

[1] ravi.ravi.viveki@gmail.com

[2] chougulenk@gmail.com

[#12] Automotive Technology, Mechanical Engineering Department, Pune University College of Engineering Pune 411005, India

ABSTRACT

Reduction of drag is becoming a very important challenge for all the automobile manufacturers as they are competing intensely to produce passenger cars with better gas mileage. Lower drag provides better performance such as higher top speed and better stability. The body shapes of passenger cars are primarily designed to meet the top speed, economical, and aesthetic requirements. Studying flow over passenger car is costly in wind tunnel due to cost for the setup as well as the number of runs required for successful drag reduction and optimization. With the use of CFD these costs are avoided and multiple runs can be set up at the same time for comparison and optimization. It is motivated for this study by using a CFD approach to analyse the flow over a MIRA reference car. In order to reduce the aerodynamic drag of cars, modification in roof is done on the baseline model and three parameters like velocity, thickness to chord ratio and position of thickness to chord ratio are used for the optimization purpose to reduce drag using Taguchi method and air flow will be simulated. After simulation it has been found that drag coefficient reduced by 2.5% and with less than 1% increment in drag. The objective of this study is to quantify effect of roof curvature on the drag and understand the mechanisms of drag production.

Keywords: Computational Fluid Dynamics, Optimization, Taguchi Method, Drag Coefficient.

ARTICLE INFO

Article History

Received : 23th May, 2015

Received in revised form : 25th May, 2015

Accepted : 28th May, 2015

Published online :

1st June 2015

I. INTRODUCTION

Fuel efficiency improvement in ground vehicles will continue to be a significant issue in the automobile industry. In order to increase fuel efficiency one can go with improving combustion process in the engine and other by reducing the total drag force on the vehicle in motion. The aerodynamic drag in vehicles includes pressure drag, skin friction drag, interference drag and induced drag. The form drag contributes around 60 to 65% of the total drag due to the flow separation. The separated flows in the rear of the vehicle cause pressure recovery losses and hence create vorticity, which contribute to aerodynamic drag [1]. The aerodynamic drag force is proportional to the square of the velocity and the engine power required to overcome the aerodynamic drag is a function of the cube of the velocity. More than 50% of fuel is consumed at high speeds to overcome aerodynamic drag. Hence there is much scope for reducing aerodynamic drag.

Numerical simulation of flow around bluff bodies provides a powerful tool for analysis, as experimental tests are time consuming. Computational fluid dynamics can be used to provide detailed information on drag and downforce. Aerodynamic shape optimization has been a challenging field of study in fluid dynamics. Roof curvature is important vehicle shape parameters from aerodynamic point of view. Many old car designs are with curved roof which were thought to be efficient but a thorough study to benchmark this claim has not be done up to now. Car shapes are also observed with flat roof or with slight curvature at rear end of roof. Recent change in trend urging aesthetic looks and high efficiency of the vehicles has attracted many researchers to

propose new innovative designs. With development in computational methodologies and advancement in computational resources to solve complex equations has facilitated minimized experimentation costs and improved designs. As flow over the roof affect wake region, roof shape study is important from aerodynamic point of view.

MIRA REFERENCE CAR

The MIRA reference cars were a group simplified car shapes which were evolved from work undertaken in the early 1980s when European and North American wind tunnel operators began a series of correlation exercises. Initially the model was constructed in 20%, 25%, 1/3rd and full-scale versions. In 1990s, 40% and 30% versions were added to MIRA's own collection to aid manufacturer studies in model-full to full-scale correlation. With the availability of published experimental data and the advantage of simple surface geometry, the MIRA reference car became a popular test case when CFD emerged as a tool for automobile aerodynamics [2]. In current study, MIRA reference cars with full scalehas been used for numerical simulation. The related aerodynamic parameters and wake flow were simulated in ANSYS 15.0 and validated with the research paper. The MIRA car models are simplified vehicle car models which are very close to real vehicles. The MIRA car models have wheels but do not have wheeel cavity. The bottom of the model is very smooth and the engine hood has 10 degree angle of slope. The side windows of the car models incline and the tail of model wraps upward. There are totally four forms of the MIRA car models: the notchback, the squareback, the fastback and the pickup. The notchback is used for the simulation.The full size generic car is 4.167 m long, 1.626 m wide, 1.422 m high and with a projected frontal area of 2.3121 m^2 [2]. The computational domain is a cuboid and has dimensions of 7.5m wide, 7.5m high, and 37.5m long.

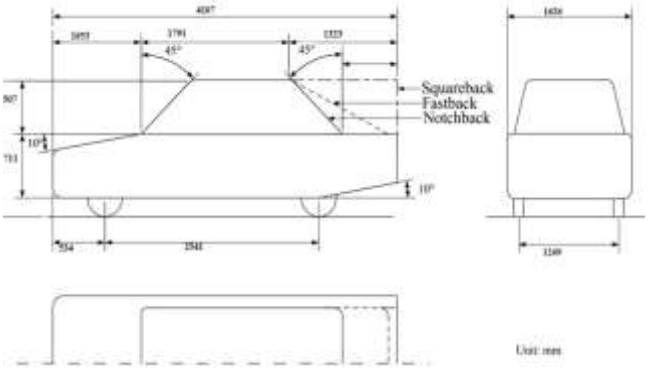

Fig.1 Dimensions of MIRA car [2].

The boundary conditions used for the analysis are uniform and steady flow with inlet velocity of 100kph, no-slip for the surface of car body and road. The sides and top of computational domain are walls with specified shear (zero Newton) and the outlet boundary is with zero gauge pressure.

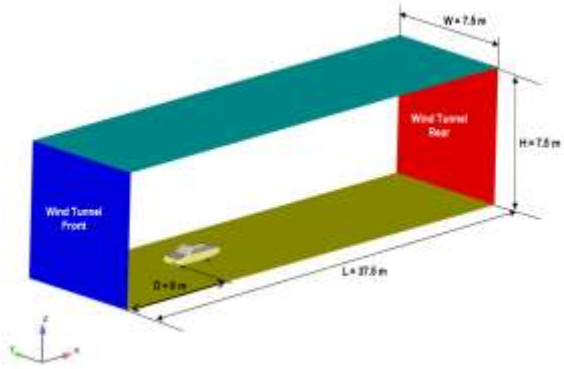

Fig.2 Dimensions of computational domain

In current computations, the unstructured hybrid mesh was generated. The surface mesh was generated using the meshing software hypermesh. In the computational domain, a small cuboid was constructed to surround the vehicle model. The volume mesh contains the hybrid Tetrahedron-Hexahedron-Pyramidal prism mesh and employed to compute the flow field around the vehicles, and the mesh was generated by ANSYS T-GRID 15.0. Eight layers of prism elements are created near the car surface in order to capture boundary layer and skin friction force with a growth ratio of 20%. The first layer height was taken as 1.4mm (30< y+ >300) . The total number of cells are approximately seven million cells. The meshed car body is then imported to Fluent 15.0.

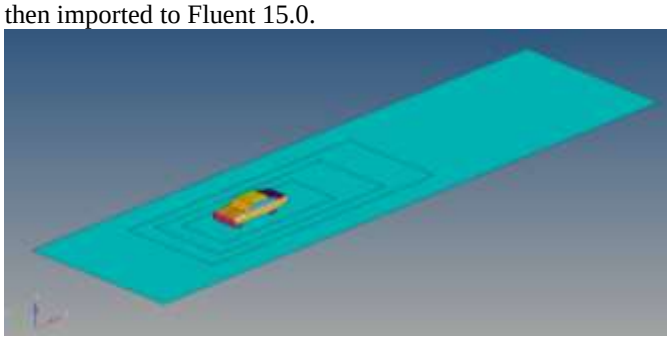

Fig.3.Domain with blocks for refinement of mesh

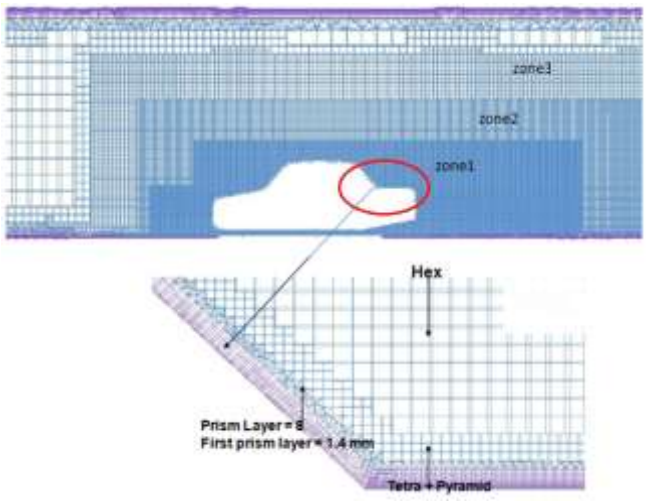

Fig. 4 Volume mesh in the symmetry plane in the vicinity of body

Below table shows the mesh refinement zones with dimensions.

Table no.1 Mesh refinement zones

Zones	Length(m)	Width(m)	Height (m)	Element Size(m)

Zone 1	6.5614	2.516	2.3599	0.015
Zone 2	8.1324	3.1671	2.9854	0.030
Zone 3	11.2602	4.4183	4.2366	0.060

NUMERICAL METHOD

Three dimensional steady incompressible viscid Reynolds Averaged Navier Stokes equations are used and RNG k-epsilon turbulence model is applied to simulate flow. The turbulence model used was more accurate for simulation and to predict the related vehicle aerodynamic parameters. In this model a new dissipation rate equation and a realizable eddy viscosity was formulated. Therefore this model is more suitable for a variety of flows, including mixing layers, shear flows, boundary layers with adverse pressure gradients inducing separation etc.
The governing equations used are,

Equation of continuity:

$$\frac{\partial(u_i)}{\partial x_i} = 0 \quad \ldots\ldots\ldots\ldots\ldots\ldots\ldots(1)$$

Equation of Reynolds-averaged Navier-Stokes equation

$$\frac{\partial(u_j u_i)}{\partial x_j} = -\frac{1}{\rho}\frac{\partial P}{\partial x_i} + \frac{\partial}{\partial x_j}(2\vartheta S_{ij} - \overline{u_i' u_j'}) \ldots\ldots (2)$$

Equation of turbulent kinetic energy (k) :

$$\frac{\partial(u_j k)}{\partial x_j} = -\overline{u_i' u_j'}\frac{\partial u_i}{\partial x_j} - \varepsilon + \frac{\partial}{\partial x_j}[(\vartheta + \frac{\vartheta_T}{\sigma_k})\frac{\partial k}{\partial x_j}]$$

Equation of turbulence dissipation rate (ϵ) :

$$\frac{\partial(u_j \varepsilon)}{\partial x_j} = C_{\varepsilon 1}\frac{\varepsilon}{k}(-\overline{u_i' u_j'})\frac{\partial u_i}{\partial x_j} - C_{\varepsilon 2}\frac{\epsilon^2}{k} + \frac{\partial}{\partial x_j}[(\vartheta + \frac{\vartheta_T}{\sigma_k})\frac{\partial \varepsilon}{\partial x_j}] \ldots\ldots\ldots(4)$$

$S_{ij} = (\frac{\partial u_i}{\partial x_j} + \frac{\partial u_j}{\partial x_i}) / 2$ is rate of strain tensor

$-\overline{u_i' u_j'}$ is the Reynolds stress tensor divided by density

$-\overline{u_i' u_j'}\frac{\partial u_i}{\partial x_j}$ is the shear production of turbulent kinetic energy

ϑ_T is the turbulent eddy viscosity, $\vartheta_T = \frac{C_\mu k^2}{\varepsilon}$, ϑ is kinematic viscosity.

The solution algorithm for the simulation used was the SIMPLE algorithm for the iterative solution of the steady RANS equations and the algorithm was of second–order upwind scheme in spatial discretization. The Convergence criteria has set on 10^{-4} for all variables. x, y, z velocity are converged well below 10^{-6} . And k, epsilon and continuity are below $10^{-}4$. The solution converged at approximately 11000 iterations.

BASEMODEL NUMERICAL RESULTS

Before optimizing the shape of roof, the base model is first validated. Below table shows comparison of the drag coefficient and lift coefficient obtained by experiment and the results of simulation. The present solutions for lift and drag coefficient for base model of MIRA car were found in excellent agreement with [1].

Table no.2. Numerical and Experimental results

Model	Experimental		CFD		Percentage error	
	C_D	C_L	C_D	C_L	C_D	C_L
MIRA	0.29	0.0397	0.309	0.041	6.55	3.77

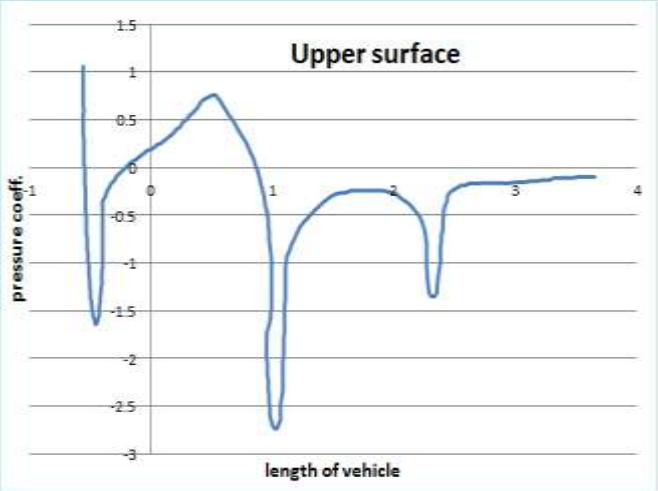

A positive pressure coefficient i.e. stagnation point Cp = 1.0 occurs in front of the car. The flow then accelerates over the bonnet and due to this the pressure drops and reaches a low value. At the intersection of the windshield and hood the flow slows down and the pressure increases. The flow then accelerates over the roof of the vehicle where the pressure drops once again and reaches a low peak value. The pressure recovered over the cabin top and pressure reached a third low point at the intersection of rear roof and rear window. Over the rear window and the luggage compartment the pressure recovered.

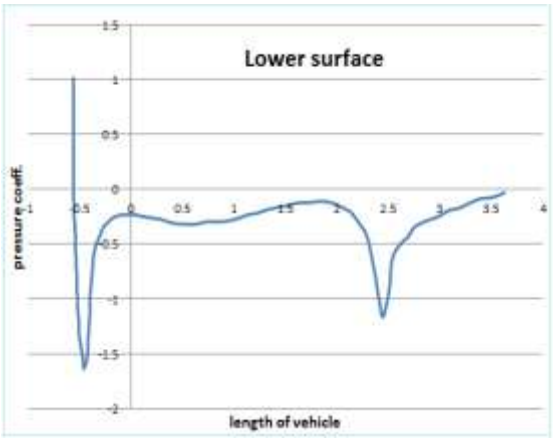

Fig. 5 Pressure coeff. Distribution in the vehicle symmetry plane.

TWO DIMENSIONAL ANALYSIS

The two dimensional simulation is carried out to optimize the roof curvature and study the flow around the body. This reduces the computational time.

The parameters used for the roof curvature optimization are the free stream velocity, thickness to chord ratio, and position of thickness to chord ratio. Here chord is the total roof length.

Table no. 3 Parameters for optimization

Velocity (kph)	t/c %	x/c %
60	2	10
80	5	30
100	10	50

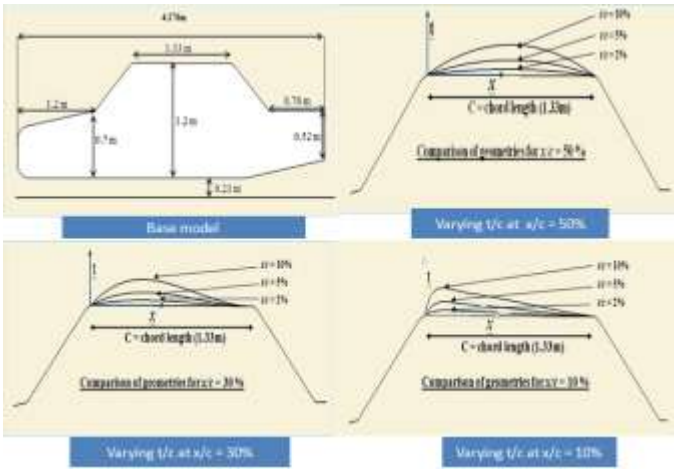

Fig.6 Different roof shapes

Hexa mesh has been generated using ICEM CFD. Fine mesh generated around the vehicle surface and at the rear of the vehicle by blockage ratio to capture the flow physics and boundary layer effects by using very small size cells and in remaining domain large cells are used as they do not affect accuracy and reduce calculation time. Boundary conditions are applied same as that applied for three dimensional.

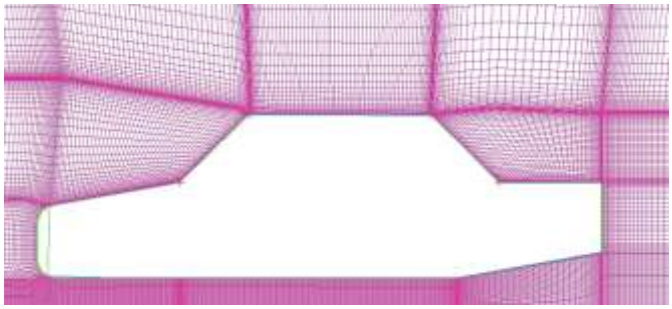

Fig.7 2-D Hexa Mesh

NUMERICAL RESULTS of 2D:

The results are discussed by plotting the pressure contours, velocity contours and streamlines showing the separation point.

Pressure contours

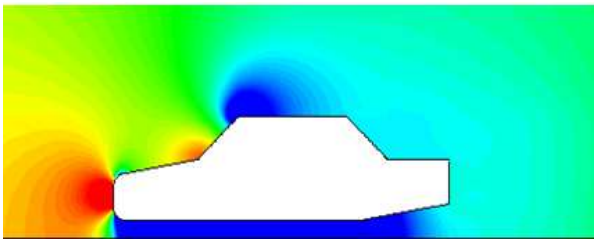

Base model

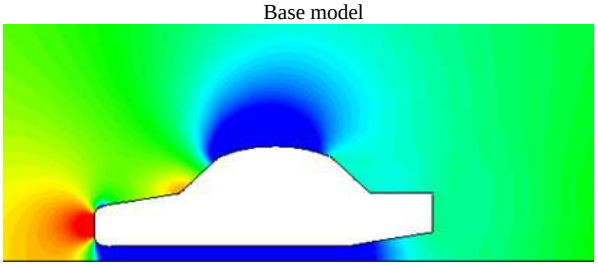

Case 1

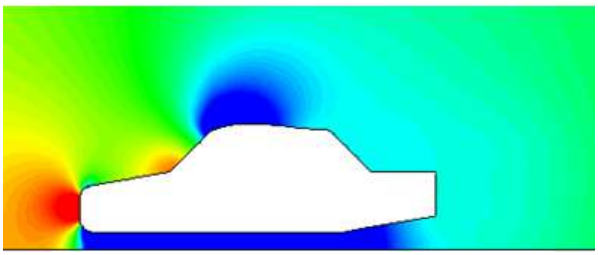

Case 2

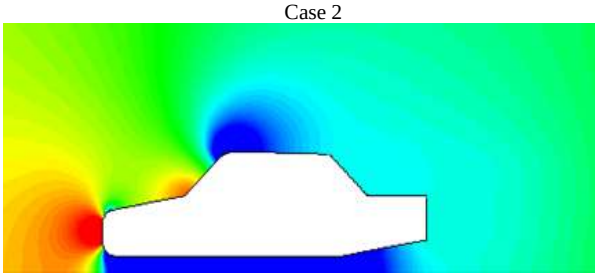

Case3

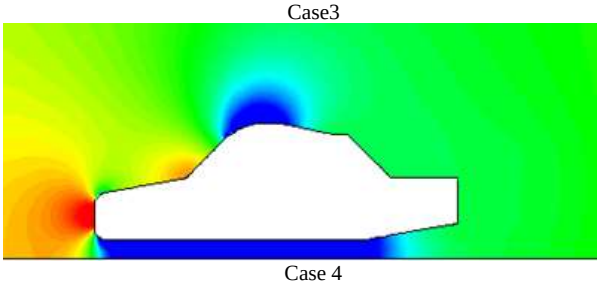

Case 4

.

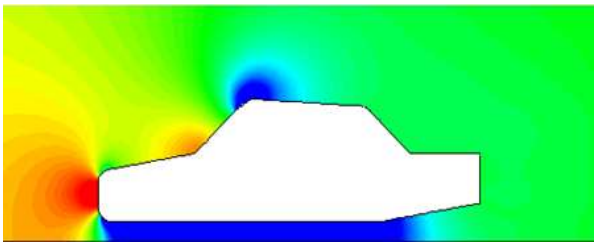

Case 5

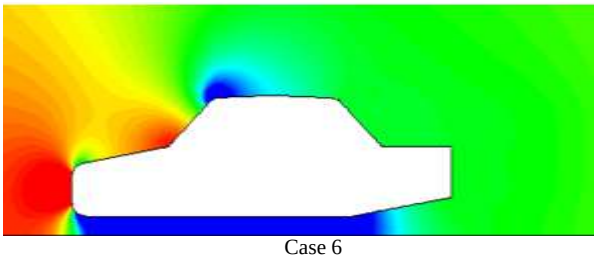

Case 6

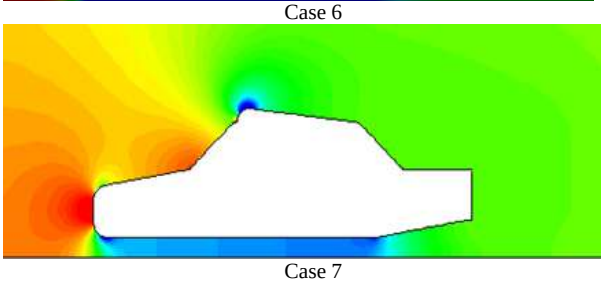

Case 7

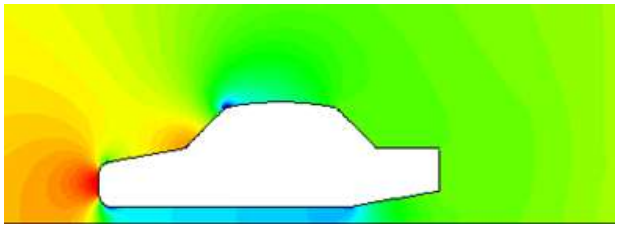

Case 8

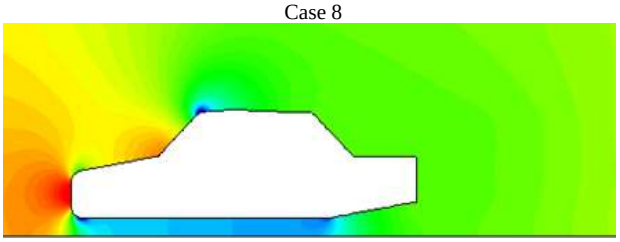

Case 9

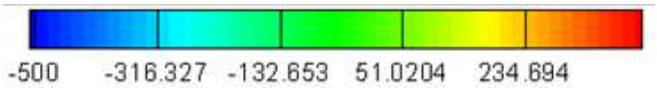

Fig.8 Pressure contours

In all the cases, at front of the car the stagnation point occurs. At the intersection of the windshield and hood the pressure increases. At the leading edge of roof the pressure decreases since the flow accelerates over the roof. In case 1,2,3,4,5,6 and basemodel, under the car body much lower pressure is observed due to the high inlet velocity. Also at the rear of the car lower pressure is observed but in case 1 there is higher pressure compared to other cases. But in case 7,8 and 9 due to low inlet velocity the flow remains attached to the body and has higher pressure at rear as flow is viscously dominant. Case 1 shows the better results as compared to other.

Velocity contours

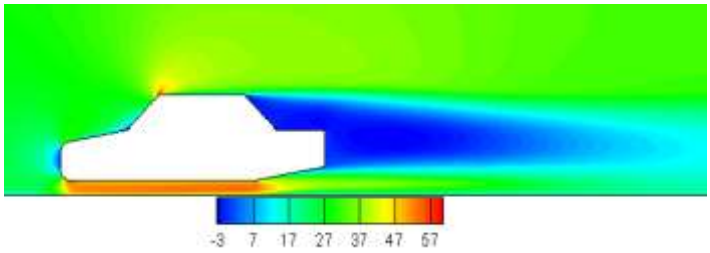

Basemodel

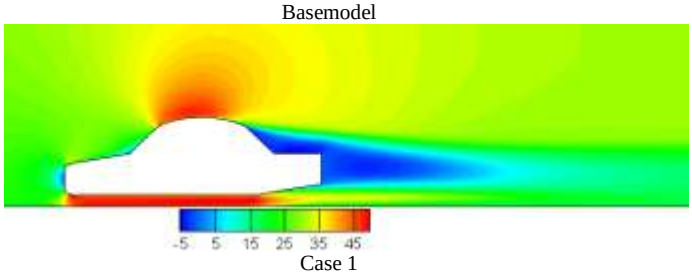

Case 1

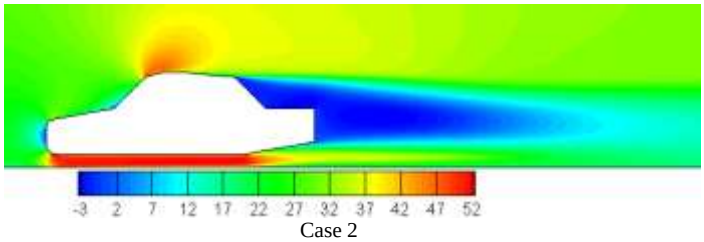

Case 2

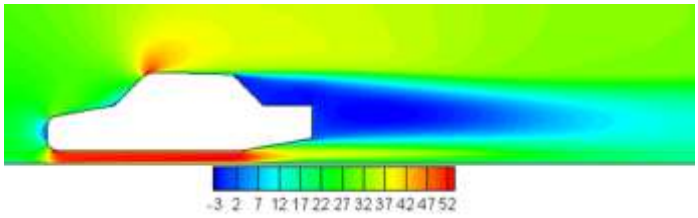

Case 3

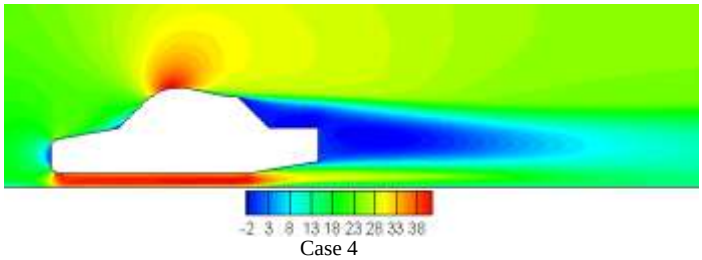

Case 4

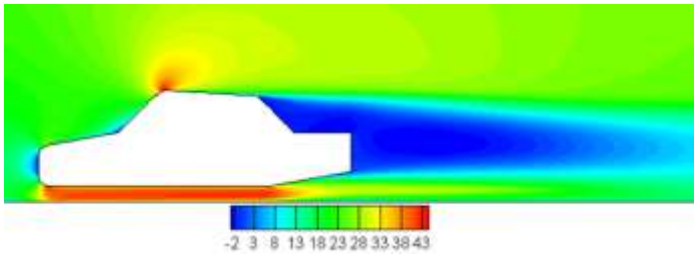

Case 5

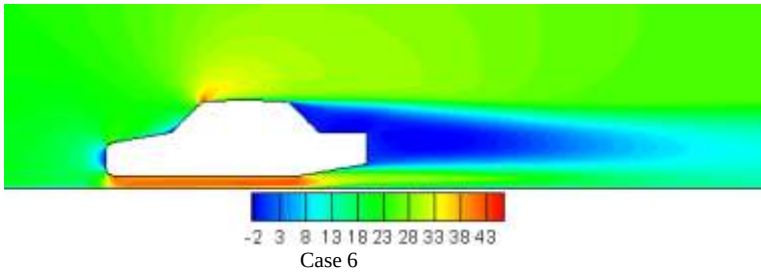

Case 6

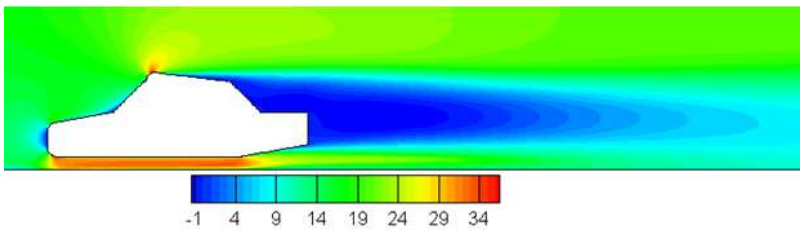

Case 7

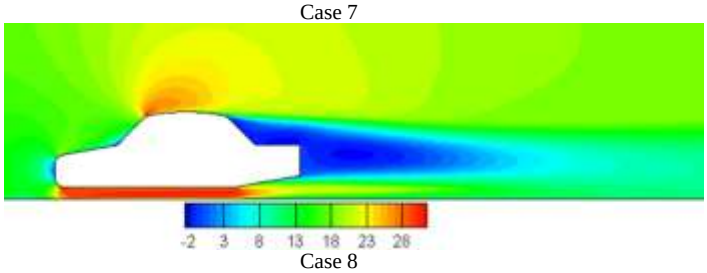

Case 8

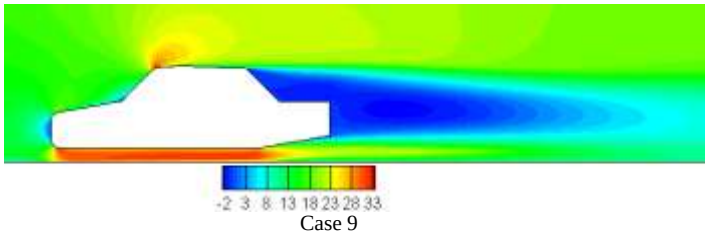

Case 9

Fig.10 Velocity contours

From the velocity contours it can be seen that the low velocity zone is generated at the rear side of vehicle. This gives the data about the wake region formed at the rear of the vehicle. In case1 the wake region formed is less as compared to other cases. Case 7,8,9 has less inlet velocity but the wake formed is higher and has much low velocity. This increases the drag force of the vehicle. Below table shows the drag and lift force values obtained from numerical simulation.

Table No. 4 Drag and Lift force values

Sr.No.	Velocity (Kmph)	t/c %	x/c %	Drag force (N)	Lift force (N)
1	100	10	50	245.37	1676.61
2	100	5	30	421.92	2715.65
3	100	2	10	446.84	2901.31
4	80	10	30	257.93	1515.07
5	80	5	10	292.09	1766.36
6	80	2	50	245.68	1759.18
7	60	10	10	223.84	1143.26
8	60	5	50	152.60	994.44
9	60	2	30	175.09	1098.26
Basemodel	100	0	0	473.62	1605.29

ANALYSIS USING TAGUHCI METHOD

The results for various combinations of models were obtained by numerical simulation as per the orthogonal array. The numerical results were analyzed using the commercial software MINITAB 14 specifically used for design of experiment applications. To measure the quality characteristics, the numerical values are transformed into signal to noise ratio. For present work 'smaller the better' was used. This is because we need a drag force lower value so that the performance of vehicle is improved. The S/N ratio for this drag force needs to be smaller. From the above graph the minimum drag value for velocity occurs at 100, t/c occurs at 10, and x/c occurs at 50. The final optimized parameters for are velocity of 100 kph, thickness to chord ratio 10%, and position of thickness to chord ratio at 50%.

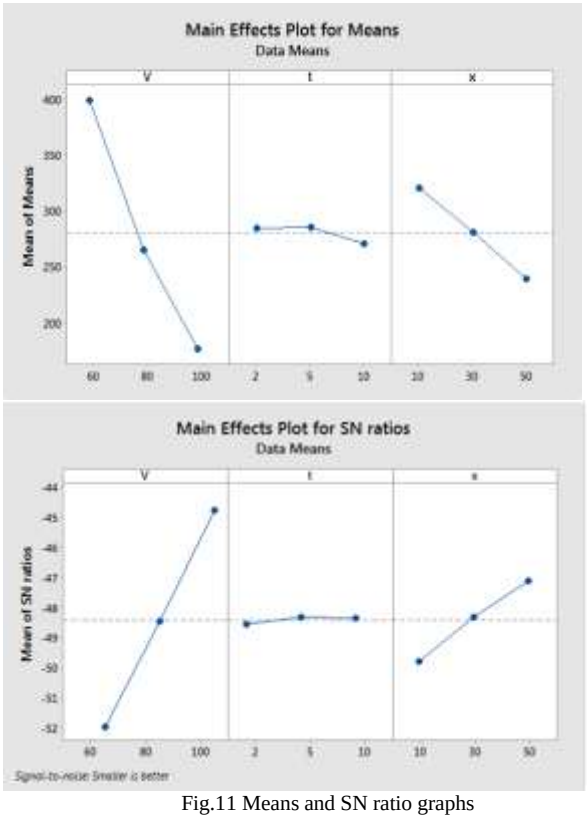

Fig.11 Means and SN ratio graphs

For present work 'smaller the better' was used. This is because we need a drag force lower value so that the performance of vehicle is improved. The S/N ratio for this drag force needs to be smaller. From the above graph the minimum drag value for L1 occurs at 100, L2 occurs at 10, and L3 occur at 50. The final optimized parameters for are velocity of 100 kph, thickness to chord ratio 10%, and position of thickness to chord ratio at 50%.

Comparison of results between the Base model and Optimized model

The 3-d results shows the clear picture of the flow around the vehicle. The pressure contours, velocity contours and the total null pressure iso-surface plots are plotted below and analysed it.

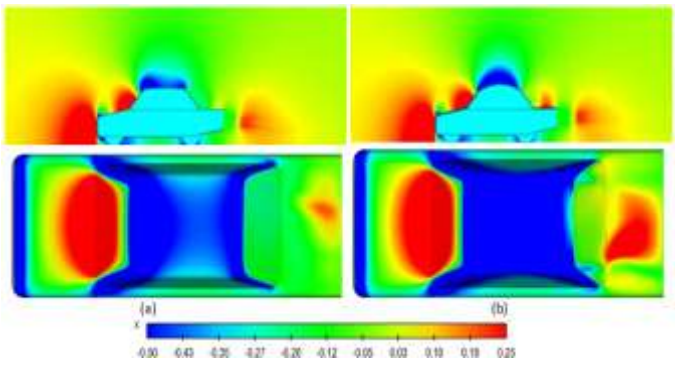

Fig.12 Pressure coefficient contours

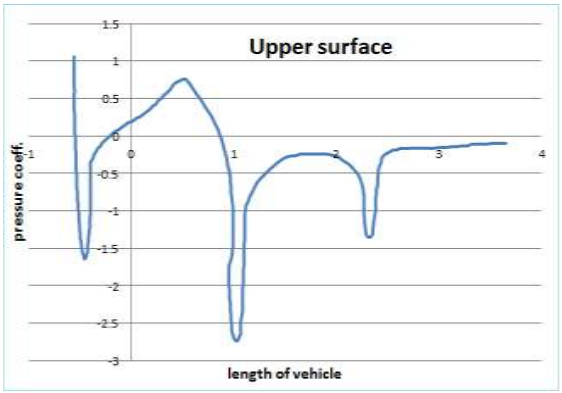

Fig.13 Pressure coefficient distribution for base model

.

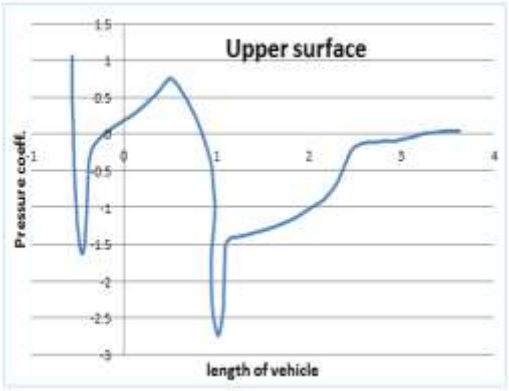

Fig. 14 Pressure coefficient for Optimized model

As roof curvature increases, low pressure is observed on roof. In base model, more pressure is observed on roof compared to optimized case. It is due to flow acceleration at

front of roof. It will have effect on lift performance of vehicle. To prevent lift deterioration, roof curvature should be such that flow remain attached to roof. This can be achieved by giving curvature to rear part of roof and keeping front part of roof flat. Also there is higher pressure on optimized shape at the rear of the vehicle

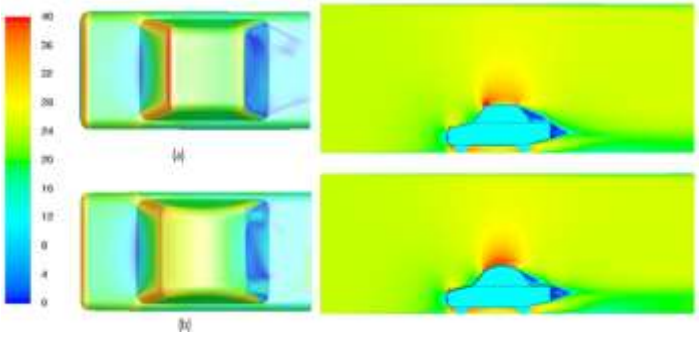

Fig.15 Velocity contours

The low zone velocity is reduced at the rear of the windscreen as can be seen from above velocity contour. Hence this reduces the wake region. Hence less drag force is generated.

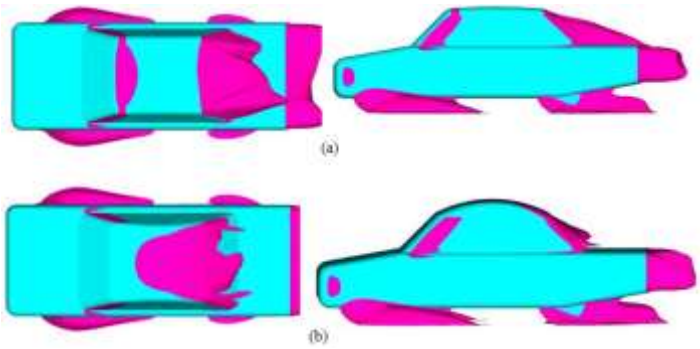

Fig. 16 Null total pressure iso- surface plots.

Fig. shows null total pressure Iso-surface for base model and optimized model. Total Pressure is combination of static as well as dynamic pressure. Null total pressure gives an idea about flow separation and wake size. Above plot shows that, as curvature is increased, tendency of flow attachment is increasing on rear wind screen. But flow starts separating on roof itself. We always recommend to have flow attached to surface so to reduce drag. Hence roof curvature will give advantage at rear because of flow attachment but separation at front of roof will deteriorate aerodynamic performance. Flow attachment is observed on rear windscreen, hence reduces separation. Other separation is observed on wheels, A pillar etc.

NUMERICAL RESULTS

Table no.5 Numerical Results

Model	C_D	C_L	% decrease in C_D	% increment in C_L
Baseline	0.309	0.04121	0	0
Optimized model	0.301	0.04163	2.58 %	0.97 %

CONCLUSION

The study carried out the flow over the baseline MIRA car and also with various roof curvature shapes. Pressure and velocity contours help to analyze the flow structure over the baseline and optimized shape. Various designs of experiments were carried out and simulated in order to get the optimized shape to reduce the drag coefficient. The analysis of all these models give the flow structure of air over the car. From the above results it was observed that as roof curvature increases from the mid position of roof, wake zone reduces hence vehicle drag coefficient reduces by 2.58%. Roof curvature will lead to more low pressure zone above roof and this will lead to more lift and was found to be less than 1%. More lift will lead to less vehicle stability at higher speed. So we have optimized between drag reduction and lift increment. More the smooth curvature, more the drag reduction.

REFRENCES

[1] Y. Wang, Y. Xin, Zh. Gu, Sh. Wang, Y. Dengand X. Yang, "Numerical and Experimental investigations on the aerodynamic characteristic of three typical passenger vehicles", Journal of Applied Fluid Mechanics, 2014 Vol. 7, No. 4, pp. 659-671.

[2] J. S. Rao, M. Sarvanakumar and D.C.Vijay Chandar, "External Aerodynamic Flow for High Speed Passenger Car", SAE Paper No. 2007-26-050.

[3] Geoffrey M. Le Good, Kevin P. Garry, "On The Use Of Reference Models In Automotive Aerodynamics", SAE Technical Paper 2004-01-1308.

[4] Inchul Kim, Hualei Chenand Roger C.Shulze, " A rear spoiler of a new type that reduces the aerodynamic forces on a Mini Van", SAE Technical Paper 2006-01-1631.

[5] Adrian P. Gaylard and Nicholas Oettle, "Evaluation of Non-Uniform Upstream Flow Effects on Vehicle Aerodynamics", SAE International 2014-01-0614.

[6] Frank M.WHITE, "Fluid Mechanics", Fourth Edition University of Rhode Island

[7] Makowski, F.T. and S.E., Kim, "Advances in External-aero Simulation of Ground Vehicles using the Steady RANS Equations", SAE Paper No. 2000-01-0484

[8] Scott Wordley and Jeff Saunders Monash Wind Tunnel, "Aerodynamics for Formula SAE: Initial design and performance prediction", SAE Paper No.2006-01-0806

[9] Takayoshi Nasu and Yoshimitsu Hashizume2014 , " Study on the transient behaviour of the vortex structure behind Ahmed body", SAE Technical Paper 2014-01-0597.